nature climate change

SUPPLEMENTARY INFORMATION

DOI: 10.1038/NCLIMATE1433

Black-carbon reduction of snow albedo

OL Hadley & TW Kirchstetter

Table of Contents

Section 1: Aqueous suspensions of black carbon (BC) 2

Section 2: BC concentration in melted snow 2

Section 3: Mass absorption cross-section (MAC) of BC in air 3

Section 4: Snow Grain Shape and Effective Radius 3

Section 5: Minimizing error in snow albedo measured using an integrating sphere-equipped spectrometer 4

Section 6: Adjusting for light lost to the snow sample holder during albedo measurements 5

Section 7: Snow Ice and Aerosol Radiation (SNICAR) model 7

Supplementary References 8

Supplementary Figures 10

Section 1: Aqueous suspensions of black carbon (BC)

The BC used to contaminate laboratory snow was generated with an inverted diffusion flame of methane and air[1] and collected onto Teflon membrane filters. Figure S1 shows the size distribution of the BC in air. BC laden filters were exposed to ozone at levels in excess of 100 ppm for 20 minutes, which transformed the BC from hydrophobic to hydrophilic[2,3]. Following ozone exposure, each filter was weighed using a microbalance (Sartorius SE2-S). After weighing, the BC was rinsed with pure water from the filter into a volumetric flask. The filters were dried and re-weighed to determine the mass of BC removed. A range of precisely determined concentrations of stably suspended BC in water was used to calibrate the absorbance spectroscopy method discussed below and to make BC contaminated snow (as described in the manuscript).

Section 2: BC concentration in melted snow

BC concentration in snow samples was determined by measuring the absorbance of melted samples using a spectrometer equipped with a liquid waveguide capillary cell (LWCC). The LWCC is a meter long capillary tube coated to prevent scattered light from escaping. The LWCC replaces the cuvette typically used for absorption spectroscopy. Following the Beer-Lambert law, absorbance (A) varied in proportion to the BC concentration of prepared aqueous suspensions:

$$A = \sigma C L \qquad (1)$$

where $A = \ln(I_o/I)$, I_o and I are the intensities of light transmitted through the LWCC containing pure water and an aqueous suspension of BC, respectively, C is the BC concentration (ppm = g m^{-3}), L is the length of the LWCC (1 meter), and σ is a

proportionality constant (m^2 g^{-1}) obtained from the slope of the calibration curve (Figure S2).

Section 3: Mass absorption cross-section (MAC) of BC in air

To determine the MAC of the BC used to contaminate snow (15 ± 1 m^2 g^{-1} at 532 nm), we divided the absorption coefficient (m^{-1}) by the mass concentration (g m^{-3}) of the steady effluent of BC from the diffusion flame. Absorption coefficient was measured using a photo-acoustic instrument[4] and BC mass concentration was determined from the BC mass collected on quartz filters and measured using a thermal-optical analysis method[5].

Section 4: Snow Grain Shape and Effective Radius

Imaging laboratory snow at a magnification of 500x with a digital microscope (Dino-Lite Pro, model AM413TS), we observed that snow grains were spherical (Figure S3). Snow grain size was controlled by varying the pressures applied to the different spray nozzles used when making snow. Effective radius (R_{eff}) was determined from the spectral albedo of snow in the near-infrared. In this spectral region, the albedo of snow is very sensitive to and commonly used to determine effective radius[6-9] We measured the albedo of our snow in the wavelength range from 1000 to 2500 nm using a dual-beam spectrometer (Perkin Elmer Lambda900) equipped with a 15 cm Spectralon integrating sphere, and then we found the effective radii (55, 65, and 110 μm) for which the Snow Ice and Aerosol Radiation (SNICAR) model best simulated the measured spectra (Figure S4). The SNICAR model[10,11], which is described in SI-Section 7, was run with parameters that matched those of our albedo measurements: a solar zenith angle of 0°, a snow density of 550 kg m^{-3}, and direct light in clear sky conditions. We note that the

simulated spectral albedos of infinitely deep snow and snow with a depth of 1 cm are equivalent. This illustrates that our snow samples (5 cm deep, 5 cm in diameter) were sufficiently deep to prevent the infrared radiation from reaching the sample holder surface and biasing our measurements.

Section 5: Minimizing error in snow albedo measured using an integrating sphere-equipped spectrometer

We used an Ocean Optics USB2000+ single beam spectrometer equipped with a 15 cm diameter, integrating sphere (Sphere Optics SPH-6Z-4) to measure snow albedo. The integrating sphere is coated with Zenith UltraWhite, a highly Lambertian material with >98% reflectance from 300 to 2000 nm and an average reflectance of >95% over the solar spectrum. The reflectance standard (Sphere Optics, model SG 3088 Zenith Reflectance Standard 99%) we used is made of the same material and came supplied with calibration data specifying the true reflectance of the standard at each wavelength between (250 – 2500 nm), traceable to NIST standards. The following describes the integrating sphere configuration and steps taken to reduce measurement error.

1) To avoid the substitution error associated with a single beam integrating sphere[12], we used the comparison method to measure snow albedo[13]. The substitution error is inherent in single beam integrating spheres that measure reflectance. It is caused by the difference in the throughput of the sphere when the reference (i.e., the reflectance standard) makes up a portion of the sphere wall and when a sample of different reflectance is substituted for the reference. In the comparison method, one spectrometer scan is recorded when the reference is at the sphere's reflectance port and the sample is at a port that is normal to the reflectance port (Figure S5b). The positions of the sample and

reference are swapped and a second scan is recorded (Figure S5a). Therefore, the average reflectance and throughput of the sphere remain unchanged from the reference to the sample scan.

2) One potential source of bias in our snow albedo measurements the emergence of reflected radiation to the exterior surface of the sphere rather than into the sphere's reflectance port. Another is the absorption of radiation that reaches the snow sample holder. To minimize the loss of light to the exterior of the integrating sphere and to the snow sample holder, the area of the collimated light incident on snow samples (0.27 cm^2) was kept small compared to the area of the reflectance port (11.45 cm^2) and sample holder (20.3 cm^2). Also, snow samples were densely packed to maximize the optical depth and reduce the distance that radiation traveled in the snow sample holder (see SI-Section 6).

3) A baffle was installed inside the sphere between the sample port and the sphere wall opposite the fiber-optic port to prevent detection of specular components of light reflected from snow samples. While snow reflectance is approximately Lambertian, specular reflectance of wavelengths greater than 700 nm have been reported[6]. Compared to diffusely reflected light from the Lambertian reflectance standard, the intensity of specular components of reflected light from snow would be more intense, and this could potentially bias snow albedo measurement. A baffle between the sample and fiber-optic ports was unnecessary because the narrow viewing angle of the fiber prevented detection of possible specular components of reflected light.

Section 6: Adjusting for light lost to snow sample holder during albedo measurements

Snow was densely packed (550 kg m^{-3} versus a typical value of 200 kg m^{-3} for natural snow) into a sample holder (5 cm deep, 5 cm in diameter) aiming to maximize optical depth and minimize the fraction of radiation incident on the snow's surface that reached and, thus, would be absorbed by the holder (which was black in color). A small fraction of the incident light did, however, penetrate the snow and reach the holder, which biased low the measured snow albedo. To remove the influence of the sample holder, all values of measured snow albedo were multiplied by the wavelength-, snow grain size-, and BC content-specific values shown in Figure S6. The resulting (i.e., adjusted) albedo values reported in this manuscript are, therefore, representative of snow of infinite depth.

The values in Figure S6 are the ratio of the albedo of infinitely deep snow to the albedo of snow with a density of 550 kg m^{-3}, a depth of 2 cm, and an underlying black surface (matching our experimental conditions). The albedo of infinitely and 2 cm deep snow was estimated using the SNICAR model, run with snow grain sizes and BC concentrations that matched those of our experiments. Two centimeters is the depth our snow samples would be if their volume was spread evenly over the surface area of the sample holder.. The largest albedo adjustment (an increase of ~6% in the visible spectral region) corresponded to pure snow with 110 μm R_{eff} (Figure S6). Smaller albedo adjustments were necessary for 65 and 55 μm R_{eff} pure snow (increases of ~3% and 1%, respectively). The albedo of BC contaminated snow samples was generally adjusted by less than 1%, arguably not significant given the uncertainty in our albedo measurements (Figures 1 & 2). These adjustments yield albedos for pure snow that closely agree with those simulated by SNICAR, consistent with previous studies that have verified the

accuracy of radiation transfer models of pure snow. The smaller adjustments needed for snow with smaller grains and for BC contaminated snow are intuitively correct because smaller grains and BC contamination increase optical depth. The very small adjustment needed for BC contaminated snow samples indicates that the optical depth was sufficiently high to prevent a significant fraction of incident light from reaching the sample holder. In all cases, the correction factor was very small in the infrared spectral region where snow is strongly absorbing.

Section 7: Snow Ice and Aerosol Radiation (SNICAR) model

SNICAR calculates snow albedo as the ratio of the upward and downward flux at the snow surface. In this study, SNICAR parameters were set to match our method of albedo measurement: direct sunlight, solar zenith angle of 0°, and clear sky conditions. The surface incident solar flux used by SNICAR was produced with the atmospheric Shortwave Narrowband Model (SWNB)[14,15]. This surface spectrum is identical to the surface solar spectrum[16] we used to calculate the albedos shown in Figure 2. The radiative transfer solution is a single-layer version of the multiple scattering, multi-layer, approximation described by *Toon et al.* (1989)[17], with the delta-hemispheric mean approximation[10]. Snow is treated as a log-normal distribution of ice spheres. Mie parameters are calculated off-line at high spectral resolution for lognormal distributions of ice spheres with effective radii ranging from 30 to 1500 μm[11]. Broadband albedo is weighted by the incident solar flux[11].

SNICAR assumes a log-normal size distribution of BC with a median radius of 0.05 μm and a standard deviation of 1.5. The index of refraction of the BC was taken from Chang and Charalampopoulos [1990][18] and varies with wavelength. At 540 nm, the

specified refractive index of BC is 1.77 - 0.63i. Using the prescribed size distribution, refractive index, and Mie theory, the BC particle mass density is tuned to obtain a spectrally resolved mass absorption cross section (MAC), which has a default value of 7.5 m^2 g^{-1} at 550 nm. Thus for a given BC mass concentration in snow, the model computes the appropriate number concentration with the previously mentioned physical and optical properties. To scale the MAC to larger and smaller values, the mass extinction cross-section (across the spectrum) is multiplied by a constant scalar specified by the user. Since single-scatter albedo remains constant, this operation scales the mass absorption cross-section by the same factor.

Supplementary References:

1. Kirchstetter, T.W. & Novakov, T. Controlled generation of black carbon particles from a diffusion flame and applications in evaluating black carbon measurement methods. *Atmospheric Environment* **41,** 1874-1888 (2007).

2. Akhter, M.S., Chughtai, A.R. & Smith, D.M. Spectroscopic Studies of Oxidized Soots. *Applied Spectroscopy* **45,** 653-665 (1991).

3. Chughtai, A.R., Brooks, M.E. & Smith, D.M. Hydration of black carbon. *Journal of Geophysical Research-Atmospheres* **101,** 19505-19514 (1996).

4. Arnott, W.P. *et al.* Photoacoustic and filter-based ambient aerosol light absorption measurements: Instrument comparisons and the role of relative humidity. *Journal of Geophysical Research-Atmospheres* **108,** 4034, doi:4010.1029/2002JD002165 (2003).

5. Kirchstetter, T.W., Corrigan, C.E. & Novakov, T. Laboratory and field investigation of the adsorption of gaseous organic compounds onto quartz filters. *Atmospheric Environment* **35,** 1663-1671 (2001).

6. Aoki, T. *et al.* Effects of snow physical parameters on spectral albedo and bidirectional reflectance of snow surface. *Journal of Geophysical Research-Atmospheres* **105,** 10219-10236 (2000).

7. Brandt, R.E., Warren, S.G. & Clarke, A.D. A controlled snowmaking experiment testing the relation between black-carbon content and reduction of snow albedo. *Journal of Geophysical Research-Atmospheres* **116**(2011).

8. Wiscombe, W.J. & Warren, S.G. A Model for the Spectral Albedo of Snow .1. Pure Snow. *Journal of the Atmospheric Sciences* **37,** 2712-2733 (1980).

9. Grenfell, T.C., Warren, S.G. & Mullen, P.C. Reflection of Solar-Radiation by the Antarctic Snow Surface at Ultraviolet, Visible, and near-Infrared Wavelengths. *Journal of Geophysical Research-Atmospheres* **99,** 18669-18684 (1994).

10. Flanner, M.G., http://snow.engin.umich.edu/.

11. Flanner, M.G., Zender, C.S., Randerson, J.T. & Rasch, P.J. Present-day climate forcing and response from black carbon in snow. *Journal of Geophysical Research-Atmospheres* **112,** - (2007).

12. Gallet, J.C., Domine, F., Zender, C.S. & Picard, G. Measurement of the specific surface area of snow using infrared reflectance in an integrating sphere at 1310 and 1550 nm. *Cryosphere* **3,** 167-182 (2009).

13. Workman, J. & Springsteen, A.W., *Applied Spectroscopy: a compact reference for practitioners*. (Academic Press, San Diego, CA, 1998).

14. Stamnes, K., Tsay, S.C., Wiscombe, W. & Jayaweera, K. Numerically Stable Algorithm for Discrete-Ordinate-Method Radiative-Transfer in Multiple-Scattering and Emitting Layered Media. *Applied Optics* **27,** 2502-2509 (1988).

15. Zender, C.S. *et al.* Atmospheric absorption during the Atmospheric Radiation Measurement (ARM) Enhanced Shortwave Experiment (ARESE). *Journal of Geophysical Research-Atmospheres* **102,** 29901-29915 (1997).

16. Levinson, R., Akbari, H. & Berdahl, P. Measuring solar reflectance-Part II: Review of practical methods. *Solar Energy* **84,** 1745-1759 (2010).

17. Toon, O.B., Mckay, C.P., Ackerman, T.P. & Santhanam, K. Rapid Calculation of Radiative Heating Rates and Photodissociation Rates in Inhomogeneous Multiple-Scattering Atmospheres. *Journal of Geophysical Research-Atmospheres* **94,** 16287-16301 (1989).

18. Chang, H. & Charalampopoulos, T.T. Determination of the Wavelength Dependence of Refractive-Indexes of Flame Soot. *P Roy Soc Lond a Mat* **430,** 577-591 (1990).

Supplementary Figures

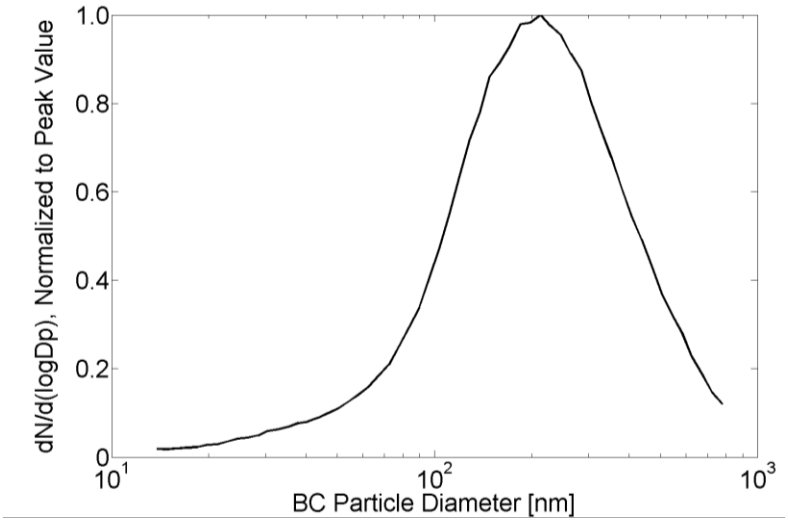

S1. Normalized size distribution of the flame-generated BC in air.

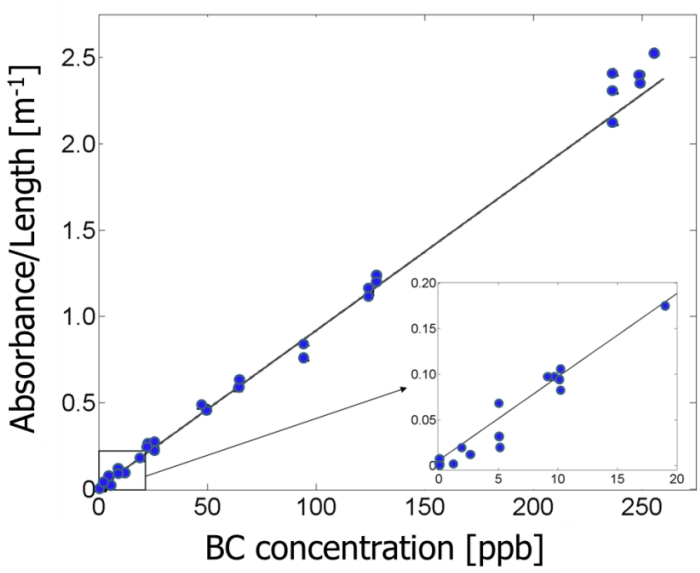

S2. Linear relationship between absorbance and BC concentration in water used to estimate BC concentration in melted laboratory snow samples. Absorbance measurements were made at 550 nm using a spectrometer equipped with a 1 m long liquid waveguide capillary cell (LWCC).

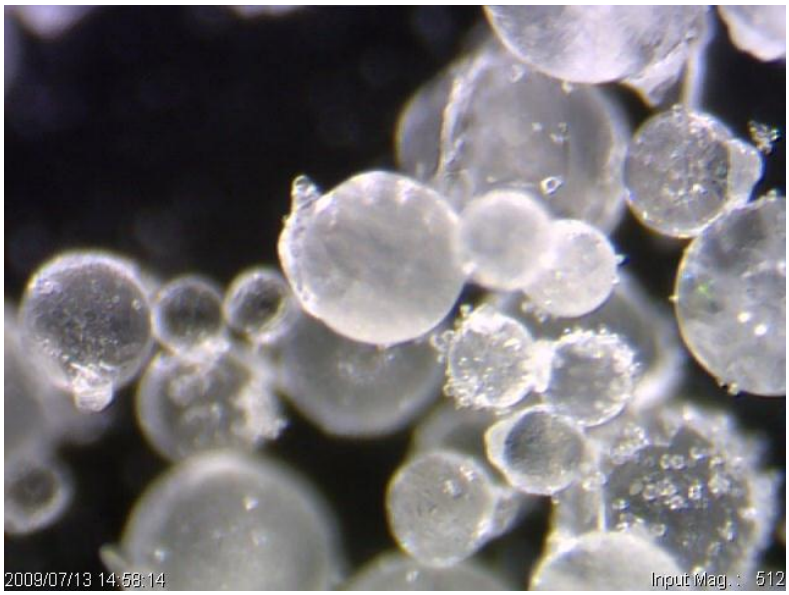

S3. Laboratory snow grains at a magnification of 500x.

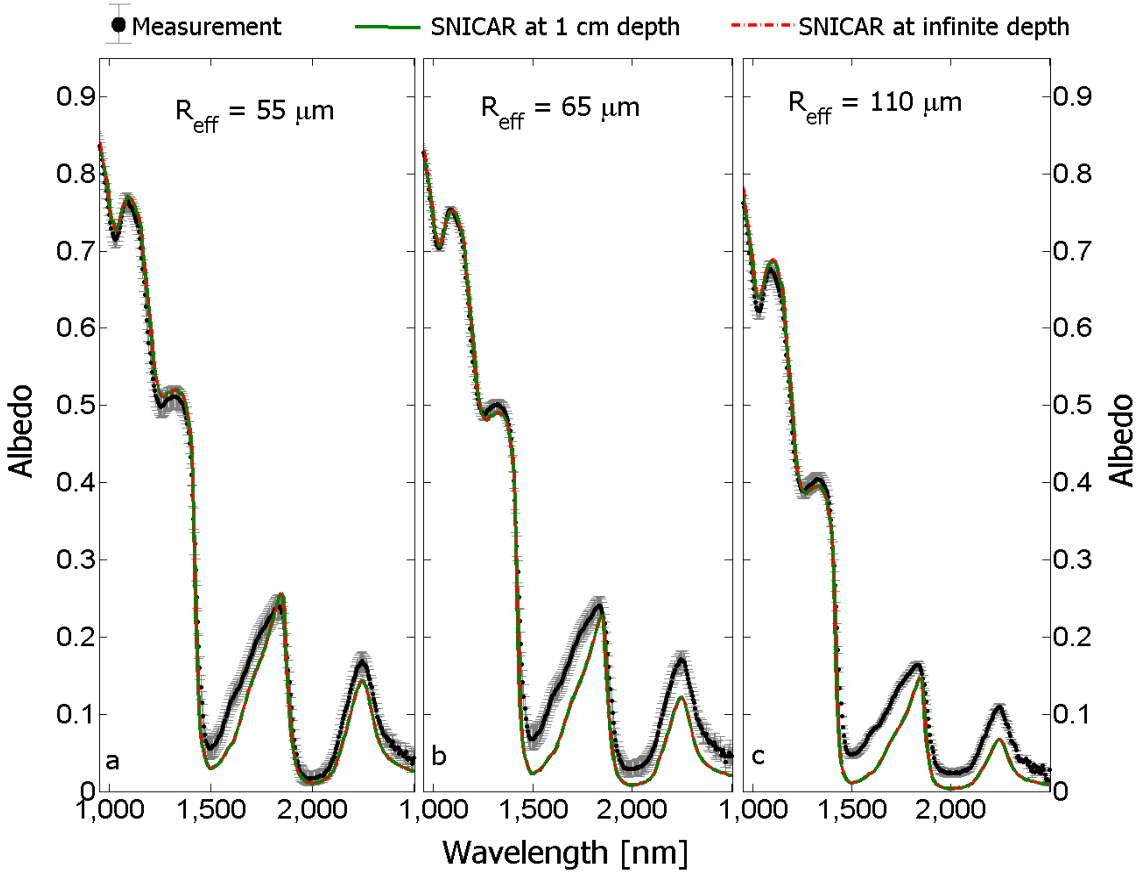

S4. Albedo of snow in the infrared spectral region (950 to 2500 nm) measured in our laboratory and matched by the SNICAR model.

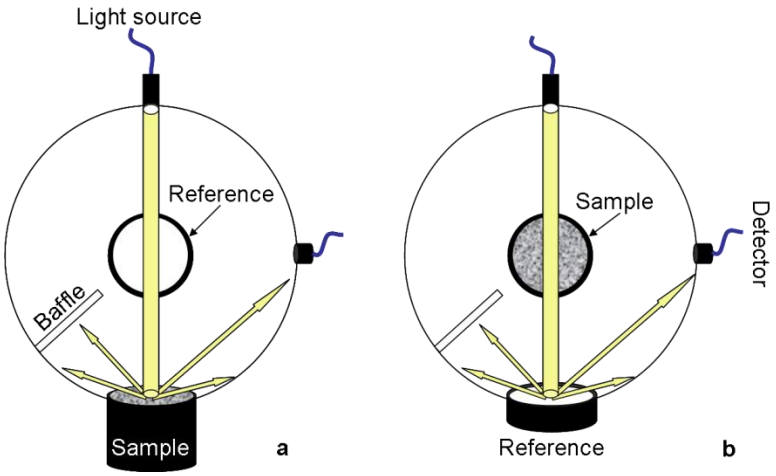

S5. The reflectance of snow samples was measured with a spectrometer equipped with an integrating sphere using the comparison method illustrated here. In this method, both reflectance standard and snow sample are placed at sphere ports when the reflectance of the (a) snow sample and (b) reflectance standard are measured.

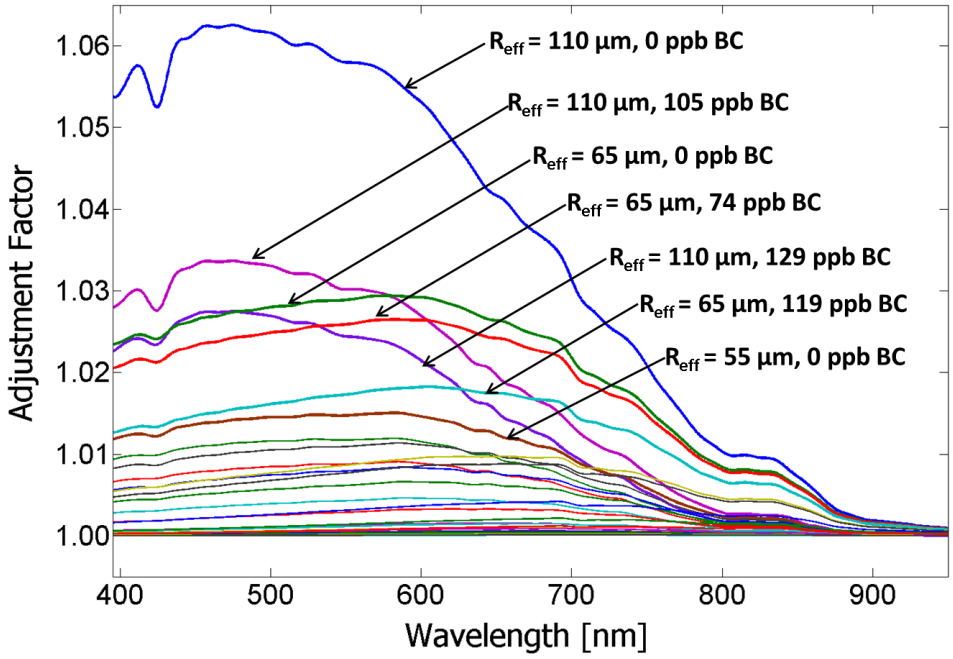

S6. Values of measured snow reflectance were multiplied by these wavelength-, snow grain size-, and BC content-specific values to correct for light lost to the snow sample cup. Values of snow albedo reported in this manuscript are, therefore, representative of snow of infinite depth.